

**Supermode spatial optical solitons in liquid crystals with competing nonlinearities**Pawel S. Jung,<sup>1,\*</sup> Wieslaw Krolikowski,<sup>2,3</sup> Urszula A. Laudyn,<sup>1</sup> Marek Trippenbach,<sup>4</sup> and Mirosław A. Karpierz<sup>1</sup><sup>1</sup>*Faculty of Physics, Warsaw University of Technology, Warsaw, Poland*<sup>2</sup>*Laser Physics Centre, Research School of Physics and Engineering, Australian National University, Canberra ACT 0200, Australia*<sup>3</sup>*Science Program, Texas A&M University at Qatar, Doha, Qatar*<sup>4</sup>*Faculty of Physics, University of Warsaw, Warsaw, Poland*

(Received 1 December 2016; published 9 February 2017)

We study numerically the formation of spatial optical solitons in nematic liquid crystals with competing nonlocal nonlinearities. We demonstrate that at a sufficiently high input power the interplay between focusing and thermally induced defocusing may lead to the formation of two-peak fundamental spatial solitons. These solitons have a constant spatial phase and hence represent supermodes of the self-induced extended waveguide structure. We show that these two-peak solitons are stable in propagation and exhibit an adiabatic transition to a single-peak state under weak absorption.

DOI: [10.1103/PhysRevA.95.023820](https://doi.org/10.1103/PhysRevA.95.023820)**I. INTRODUCTION**

Spatial optical solitons represent optical beams propagating without spreading in nonlinear media due to the balance between diffraction, which tends to spread the beam, and focusing from the nonlinear response of the medium. They have been observed in a variety of nonlinear optical materials exhibiting different types of nonlinearity, including spatially local, nonlocal, Kerr-like, or saturable [1–3]. Typically, the soliton formation has been discussed in the context of local nonlinearity, i.e., when the nonlinear response in a particular spatial location is determined by the light intensity in the very same location. The most prominent examples are the so-called Kerr media where the light-induced refractive-index change is proportional to the light intensity. In the past decade there has been interest in nonlocal nonlinear media, i.e., media with a nonlinear response (index change) at a specific point determined by the light intensity in the neighborhood of this point [4]. The spatial extent of this region relative to the soliton width determines the degree of nonlocality. The nonlocal nonlinearity has been identified in such diverse systems as thermal media [5], nematic liquid crystals (LCs) [6,7], Bose-Einstein condensates [8], and atomic clouds [9–11].

Typical fundamental bright optical solitons have the form of a finite beam, self-trapped by the nonlinear change of the polarization of the material. In this respect, in most situations, the soliton is nothing but a fundamental mode of the self-induced waveguide [12]. As such, the stationary intensity profile of a fundamental soliton features a single maximum. In principle, it is possible to form stationary multipeak solitons. However, these are not fundamental solitons. They can be realized, for instance, as vector solitons, i.e., objects formed by the simultaneous propagation of a few incoherently coupled optical beams (components), with each of them representing various (higher-order) modes of the optical waveguide induced by the total intensity. These multihumped solitons have been demonstrated in a number of systems including photorefractive and thermal media [13]. It is worth mentioning that in nonlinear media with spatially nonlocal nonlinearity, multipeak solitons

can be formed as a bound state of two or more fundamental solitons with a  $\pi$  phase shift between them. In local media out-of phase solitons tend to repel each other [1] but strong nonlocal nonlinearity introduces an attractive potential, which causes the formation of bound states of solitons [14,15]. Such dipole and higher-order multiple solitons have been observed in nematic liquid crystals and media with a thermal nonlinear response [16,17]. However, fundamental multipeak solitons have yet to be reported. While it has been shown that a model of nonlinear media with a periodic nonlocal response function supports multipeak solitons, these solitons are unstable and break up in propagation [18].

In this paper we demonstrate theoretically that fundamental two-humped spatial solitons can exist in media with competing nonlocal nonlinearities [19]. Specifically, we discuss a nonlinear model of nematic liquid crystals. We show numerically that the competition between reorientational, focusing and thermal, defocusing nonlinearities leads, in our configuration, to the formation of two-peak fundamental solitons. These solitons which can be considered as supermodes of the self-induced waveguide structure appear to be stable and resistant to strong perturbations.

**II. THEORY AND RESULTS**

We consider the propagation of an optical beam in the nematic liquid-crystal cell comprising LCs located between closely placed (tens of micrometers) parallel glass plates located in the  $y$ - $z$  plane. We assume that the internal surfaces of both plates are conditioned (for instance, by rubbing) to ensure that the molecules of the LCs are anchored and aligned at an angle  $\theta = \theta_0$ , with respect to the  $z$  axis. Hence the LC in a cell behaves as a uniaxial optical medium with a constant refractive index. The electric field of the optical beam (wavelength  $\lambda_0$ ) propagating in LC changes locally the orientation of molecules, leading to an intensity-dependent index change for extraordinary polarized light. If we consider beam propagation along the  $z$  axis, the evolution of the amplitude of electric field  $E(x, z)$  is described by [20]

$$2ik_0n(\theta_0)\frac{\partial E}{\partial z} = \frac{\partial^2 E}{\partial x^2} + k_0^2[n^2(\theta) - n^2(\theta_0)]E, \quad (1)$$

\*jung@if.pw.edu.pl

where  $k_0 = 2\pi/\lambda_0$ , and

$$n(\theta) = \frac{n_o n_e}{\sqrt{n_o^2 \sin^2 \theta + n_e^2 \cos^2 \theta}} \quad (2)$$

is an effective index of refraction for the y-polarized (i.e., extraordinary) light. Here,  $n_o$  and  $n_e$  denote ordinary and extraordinary refractive indices, respectively. The index  $n(\theta)$  depends on the local orientation of molecules, which follow the direction of the electric field of the beam, and here the molecular orientation angle  $\theta$  is governed by the following relation,

$$\frac{\partial^2 \theta}{\partial x^2} - \frac{\Delta \varepsilon \varepsilon_0}{2K} \sin 2\theta |E|^2 = 0. \quad (3)$$

Here,  $K$  is an effective elastic constant [20,21] and  $\Delta \varepsilon = n_e^2 - n_o^2$ . As Eqs. (2) and (3) show, the light-induced reorientational index change is spatially nonlocal and it is always positive as the molecules tend to align along the direction of the electric field. This leads to self-focusing of the extraordinary polarized optical beam and the formation of bright solitons, called nematicons [20,22]. In the following, we will assume that the propagation of light in the liquid crystal is accompanied by weak absorption which causes its heating. This process is governed by the heat equation

$$\kappa \frac{\partial^2 T}{\partial x^2} + \frac{c \varepsilon_0 \alpha}{2} |E|^2 = 0, \quad (4)$$

where  $T$  denotes temperature,  $\kappa$  is the thermal conductivity,  $\alpha$  is the absorption coefficient, and  $c$  is the speed of light.

The light-induced heating modifies both the ordinary and extraordinary refractive indices of the liquid crystal [23], inducing effective self-defocusing of the extraordinary polarized beam. Therefore, the nonlinear response of the nematic liquid crystal consists of two competing, spatially nonlocal processes: reorientation-driven self-focusing and thermally induced self-defocusing. It is worth mentioning that thermal nonlinearity alone can be also used to support bright solitons. This requires, however, the light beam to be ordinary polarized [24,25]. Here, we are concerned with the role of the defocusing thermal effect on the reorientational nonlinearity and consider standard nematicons, formed by extraordinary polarized light.

The temperature dependence of a wide range of nematic liquid crystals is described by universal polynomial dependence [23]. In this paper, for the sake of concreteness, we will employ an empirical polynomial formula, which accurately represents the thermal response of a 4-(trans-4'-n-hexylcyclohexyl)-isothiocyanatobenzene (6CHBT) liquid crystal in its nematic phase, in the temperature range 18–42 °C [26,27]. Details of this dependence are presented in the Appendix.

In general, the elastic constant  $K$  in Eq. (3) is also temperature dependent [21]. However, this dependence is weak and, as we checked, has no effect on our results. Hence it will be neglected in further discussions.

The stationary bright soliton solutions of the system of Eqs. (1)–(4) were found numerically with the help of the imaginary-time method [28]. We assume the stationary solution of Eq. (1) in a form  $E(x, z) = E(x) \exp(i\beta z)$ , where  $\beta$  is the propagation constant. Then, after taking  $z$  to be imaginary,  $z \rightarrow iz$ , Eqs. (1)–(4) were solved iteratively until its solution converges to the stationary solution representing

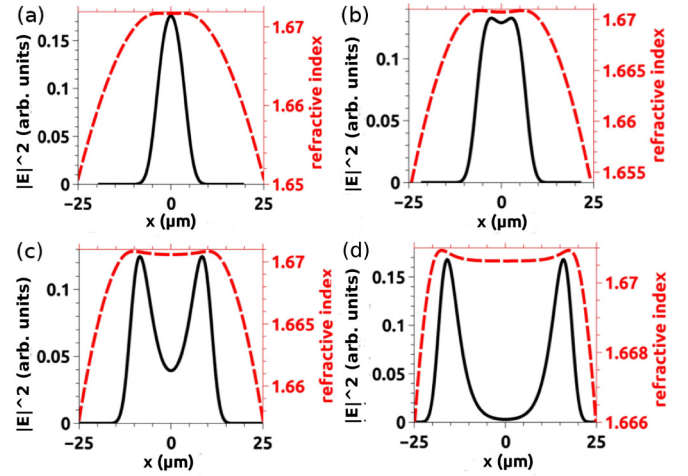


FIG. 1. Soliton solutions in the nematic liquid crystal with competing focusing and defocusing nonlocal nonlinearities as a function of beam power. Spatial intensity (solid) and light-induced refractive-index (dashed) profiles are shown [total power (a)  $P = 1.4$ , (b) 1.8, (c) 2.0, and (d) 2.2].

the fundamental soliton of the system. In these simulations the temperature and molecular orientation were kept constant at the boundaries,  $T(x = \pm x_0) = T_0 = 20^\circ$  and  $\theta(x = \pm x_0) = \theta_0 = 45^\circ$ , with  $2x_0$  being the width of the computational window. We used the finite difference to solve Eqs. (3) and (4). Our simulations show that, as long as the focusing prevails, the system always supports the existence of solitons. Typical intensity profiles of these solitons are depicted in Fig. 1, for varying total power,  $P = \int_{-\infty}^{\infty} |E(x)|^2 dx$ . In particular, for low input power, when the nonlinearity is predominantly driven by the molecular reorientation, the solitons have a typical form of a single-peak, bell-like, shape [see Fig. 1(a)]. However, as the power increases, the thermal effect becomes relevant and the soliton broadens, acquiring first a flat top [Fig. 1(b)] and eventually splitting into two distinct peaks [Figs. 1(c) and 1(d)]. It should be stressed that the two-peak solution still represents a fundamental soliton with a constant phase across the soliton. Using a waveguide analogy for solitons, for low power, the soliton-formed waveguide is induced purely by reorientation of the molecules and is smooth, a function of spatial coordinates. When the thermal effects come into play, at higher power, the waveguide structure develops two internal peaks. This is clearly seen in the refractive-index profiles plotted with a dashed line in Fig. 1. It is worth mentioning that although degrees of nonlocality represented by Eqs. (3) and (4) are comparable, they contribute differently to the resulting refractive index. The interplay between both orientational and thermal effects leads to the formation of a complex waveguide structure supporting multipeak solitons.

We can get a clearer picture of the competition between the thermal and reorientational mechanisms by utilizing the fact that the anisotropy,  $n_e^2 - n_o^2$ , is relatively small. Then, by expanding Eq. (1) in a series, we arrive at the following approximate relation for the nonlinear response,

$$\begin{aligned} n^2(T, \theta) - n^2(T, \theta_0) &= [n_e^2(T) - n_o^2(T)](\cos^2 \theta - \cos^2 \theta_0) \\ &= \Gamma(T) \Theta(\theta). \end{aligned} \quad (5)$$

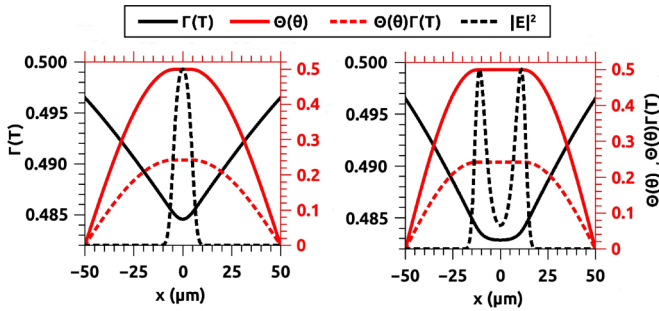


FIG. 2. Interplay between reorientational  $[\Theta(\theta)]$  and thermal  $[\Gamma(T)]$  contributions to the nonlinear response of the liquid crystal induced by two different soliton intensity distributions (indicated by the dashed line).

It appears that the nonlinearity is governed by the product of two functions representing the thermal  $[\Gamma(T)]$  and orientational  $[\Theta(\theta)]$  contributions, respectively. This interplay is different from typical nonlinear media with competing nonlinearities where different mechanisms contribute additively to the total nonlinear response. We illustrate the interplay between the thermal and reorientational effects in Fig. 2 for two examples of light intensity distributions representing single-peak [Fig. 2(a)] and two-peak [Fig. 2(b)] solitons. It is evident that while  $\Theta(\theta)$  is responsible for spatial focusing due to the light-induced reorientation of molecules of LC and reaches its maximum at the intensity maximum, the heat-induced contribution  $[\Gamma(T)]$  decreases with intensity, causing spatial defocusing. As a result, the full nonlinear response weakens and flattens in the center, and finally develops a central dip for higher intensity. This is exactly the regime where the two-peak soliton formation takes place.

In Fig. 3 we illustrate the relation between the amplitude and the power of different soliton solutions. It is clear that two-peak solitons emerge above a certain critical power. The insets in Fig. 3 show the intensity profiles of various soliton solutions.

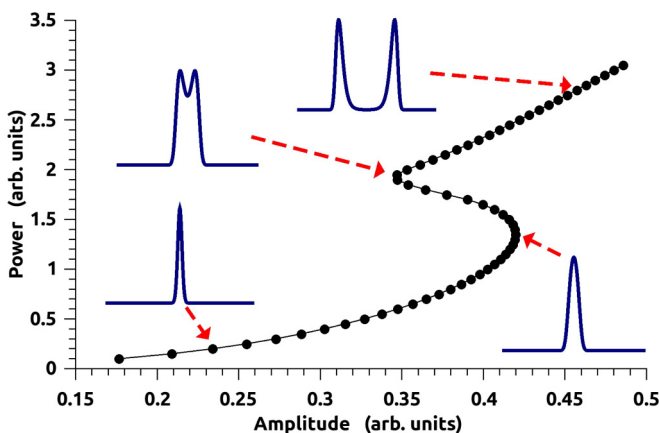


FIG. 3. Dependence of soliton power on its amplitude for wavelength  $\lambda_0 = 532$  nm and initial orientation  $\theta_0 = 45^\circ$ , background temperature  $T_0 = 20^\circ\text{C}$ , elastic constant  $K = 3.6$  pN, thermal conductivity  $\kappa = 0.135$  W/m $^\circ\text{C}$ , and absorption coefficient  $\alpha = 5.769$   $\frac{1}{m}$ .

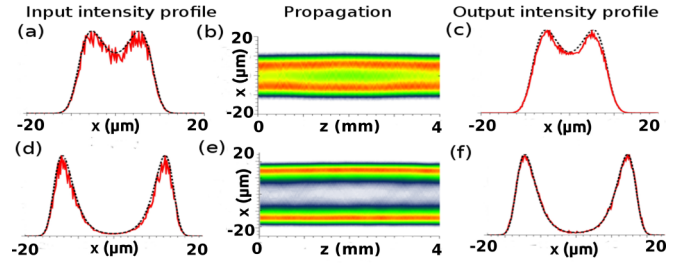


FIG. 4. Stability of two-peak solitons. (a), (d) Input intensity profiles. The red solid (black dashed) line indicates perturbed (exact) input soliton profiles; (b), (e) soliton dynamics in propagation; (c), (f) final beam profiles.

Since the bright soliton is a fundamental mode of the self-induced waveguide, one can think of these two-humped solitons as some kinds of supermodes of the self-induced waveguide structure, which are well known in the context of waveguide couplers and waveguide arrays [29]. The nonlinear version of supermodes has been also demonstrated in nonlinear couplers and cold atoms trapped in double-well potentials [30]. However, such symmetric nonlinear modes are subject to spontaneous symmetry breaking and result in spatially asymmetric intensity distributions [31,32]. Therefore, it is crucial to determine the stability of our two-peak soliton solutions. To this end we used the original system of Eqs. (1)–(4) to numerically propagate the soliton solution. We added random perturbation to the amplitude of the exact solution and propagated it over many diffraction lengths. We employed a finite-difference beam propagation method with the Runge-Kutta fourth-order algorithm and with a finite-difference relaxation with the multigrid algorithm technique. The results for two-humped solitons are shown in Fig. 4. The left (right) panel in each row shows the initial (final) intensity distribution (solid red line), while the dynamics of propagation is shown by the contour plots. It is clear that the solitons are stable in propagation and they retain their two-peak structure. Moreover, it is evident that intensity perturbation is smoothed out in propagation (compare left and right panel plots in Fig. 4). This is due to the nonlocal character of nonlinearity which tends to average out any sharp intensity variations. Additional (not shown) simulations confirm that at large angles solitons survive acute collisions with other solitons, however, in shallow angle collisions their identity is lost because the model is nonintegrable and collisions are inelastic.

So far in our simulations we have ignored linear loss. For typical experimental conditions with a propagation distance of millimeters this assumption is justified. However, it is interesting to see how the linear loss affects two-peak solitons in a long-distance propagation. We illustrate this in Fig. 5(a), where we plot the intensity evolution of an, initially exact, two-peak soliton as it propagates in the presence of weak linear loss. As its power decreases, the soliton itself undergoes an adiabatic transformation from a two-peak to a single-peak structure. At any point along its propagation the beam is, in fact, a soliton solution from the family represented in Fig. 3, as indicated by a dashed line. This is evident in Fig. 5(b), where we show the evolution of the power and amplitude of the beam during propagation.



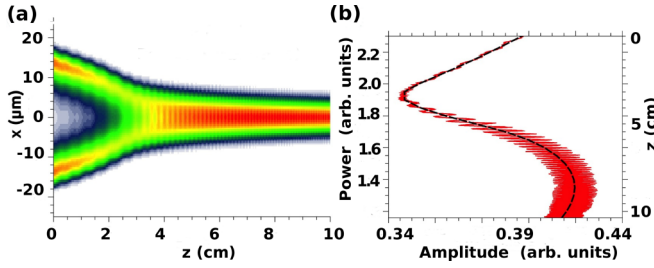


FIG. 5. Absorption-induced adiabatic transformation of a two-humped nematicon into a single-peak soliton in propagation. (a) Evolution of the beam profile. (b) Variation of the power of the soliton and its amplitude as a function of propagation distance. The dashed black line follows the stationary soliton solutions from Fig. 3.

Having in mind future experimental observations of two-humped solitons, we also address the issue of soliton excitation through proper initial conditions. In Fig. 6 we show numerically how a two-humped fundamental soliton can be created from the initial amplitude distribution given by two in-phase, weakly overlapping Gaussian beams. It is clear that the two-peak solitary beam is formed in propagation. The visible oscillations and the emission of radiation are caused by the mismatch between the exact soliton profile and input beam. Notice that unlike soliton excitation in typical nonlinear media which is accompanied by the outward emission of dispersive waves, here the radiation is confined to the center of the sample. This is because we deal here with a so-called infinitely nonlocal medium [33] where the degree of nonlocality is as large as the transverse dimension of the medium. Consequently, the light-induced waveguide is very broad, extending to the sample boundaries, imposing strong localization in the center.

### III. CONCLUSIONS

In conclusion, we studied theoretically the formation of fundamental bright solitons in nematic liquid crystals in the presence of competing nonlinearities: reorientational focusing and thermally induced defocusing. We found that for a suffi-

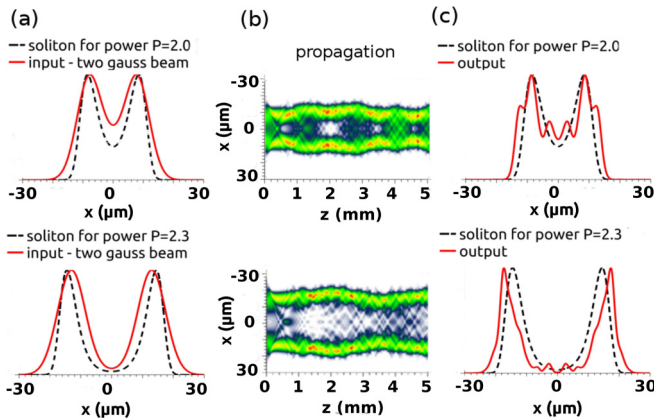


FIG. 6. Excitation of two-humped fundamental solitons. (a) Initial amplitude distribution. (b) Nonlinear evolution of the beam. (c) Output intensity distribution of the soliton. The input power  $P = 2$  (top row),  $P = 2.3$  (bottom row).

ciently large input power the system supports the formation of two-humped fundamental solitons with a uniform phase. These solitons, which could be considered as supermode solitons of the self-induced two-well index structure, appear to be stable in propagation. We also showed that these solitons could be excited by a properly shaped amplitude of the input beam. While our calculations have been conducted using parameters of a specific type of liquid crystal, our results are applicable to a wide range of nematic liquid crystals since their birefringence exhibits similar thermal behavior.

### ACKNOWLEDGMENT

This work was supported by the Qatar National Research Fund (Grant No. NPRP8-246-1-060) and the Polish National Science Centre (Grant No. UMO-2012/06/M/ST2/00479).

### APPENDIX

The ordinary and extraordinary refractive indices of the 6CHBT liquid crystal in the temperature range 18–42 °C are modeled by the following empirical relation,

$$n_o = \sum_{j=0}^3 a_j T^j, \quad n_e = \sum_{j=0}^3 b_j T^j, \quad (\text{A1})$$

where coefficients  $a_j$  and  $b_j$  are also functions of the wavelength. For instance, for  $\lambda = 532$  nm, the coefficients  $a_j$  and  $b_j$  read

$$\begin{aligned} a_0 &= 1.659, & a_1 &= 2.814 \times 10^{-3}, & a_2 &= -0.103 \times 10^{-3}, \\ b_0 &= 1.545, & b_1 &= -1.861 \times 10^{-3}, & b_2 &= 3.118 \times 10^{-5}. \end{aligned}$$

where  $T$  is expressed in degrees (Celsius).

Figure 7 illustrates the above temperature dependence. It clearly shows that while an ordinary refractive index only weakly depends on temperature, the extraordinary index decreases fast with temperature. At roughly 42 °C the crystal undergoes a phase transition from a nematic to an isotropic phase.

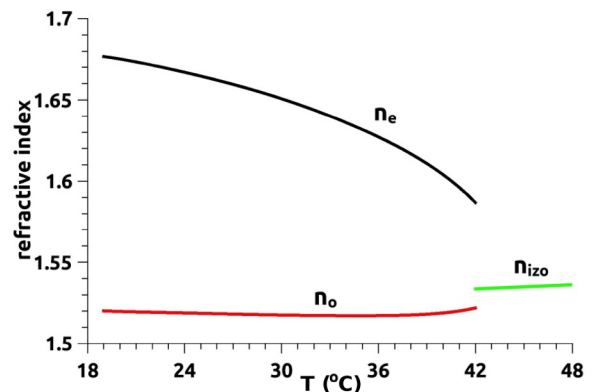


FIG. 7. Temperature dependence of ordinary ( $n_o$ ) and extraordinary ( $n_e$ ) refractive indices of the 6CHBT liquid crystal, for  $\lambda = 532$  nm.  $n_{izo}$  denotes the refractive index in the isotropic phase.

- [1] G. Stegeman and M. Segev, *Science* **286**, 1518 (1999).
- [2] Y. Kivshar and G. P. Agrawal, *Optical Solitons: From Fibers to Photonic Crystals* (Academic, San Diego, 2003).
- [3] P. Varatharajah *et al.*, *Opt. Lett.* **13**, 690 (1988).
- [4] O. Bang, W. Krolikowski, J. Wyller, and J. J. Rasmussen, *Phys. Rev. E* **66**, 046619 (2002).
- [5] F. W. Dabby and J. B. Whinnery, *Appl. Phys. Lett.* **13**, 284 (1968).
- [6] C. Conti, M. Peccianti, and G. Assanto, *Phys. Rev. Lett.* **91**, 073901 (2003).
- [7] *Nematicons: Spatial Optical Solitons in Nematic Liquid Crystals*, edited by G. Assanto (Wiley, Hoboken, NJ, 2012).
- [8] F. Dalfovo, S. Giorgini, L. P. Pitaevskii, and S. Stringari, *Rev. Mod. Phys.* **71**, 463 (1999).
- [9] D. Suter and T. Blasberg, *Phys. Rev. A* **48**, 4583 (1993).
- [10] S. Skupin, M. Saffman, and W. Krolikowski, *Phys. Rev. Lett.* **98**, 263902 (2007).
- [11] F. Maucher, T. Pohl, S. Skupin, and W. Krolikowski, *Phys. Rev. Lett.* **116**, 163902 (2016).
- [12] A. W. Snyder, D. J. Mitchell, and Y. S. Kivshar, *Mod. Phys. Lett. B* **9**, 1479 (1995).
- [13] M. Mitchell, M. Segev, and D. N. Christodoulides, *Phys. Rev. Lett.* **80**, 4657 (1998).
- [14] W. Krolikowski, O. Bang, J. Wyller, and J. Rasmussen, *Acta Phys. Pol., A* **103**, 133 (2003).
- [15] D. Buccoliero, A. S. Desyatnikov, W. Krolikowski, and Y. S. Kivshar, *Phys. Rev. Lett.* **98**, 053901 (2007).
- [16] X. Hutsebaut *et al.*, *Opt. Commun.* **233**, 211 (2004).
- [17] C. Rotschild, M. Segev, Z. Xu, Y. Kartashov, L. Torner, and O. Cohen, *Opt. Lett.* **31**, 3312 (2006).
- [18] B. K. Esbensen, M. Bache, W. Krolikowski, and O. Bang, *Phys. Rev. A* **86**, 023849 (2012).
- [19] B. K. Esbensen, A. Wlotzka, M. Bache, O. Bang, and W. Krolikowski, *Phys. Rev. A* **84**, 053854 (2011).
- [20] G. Assanto and M. Peccianti, *IEEE J. Quantum Electron.* **39**, 13 (2003).
- [21] I. Khoo, *Liquid Crystals: Physical Properties and Nonlinear Optical Phenomena*, Vol. 64 (Wiley, Hoboken, NJ, 2007).
- [22] U. A. Laudyn *et al.*, *Sci. Rep.* **6**, 22923 (2016).
- [23] J. Li, C.-H. Wen, S. Gauza, R. Lu, and S.-T. Wu, *J. Disp. Technol.* **1**, 51 (2005).
- [24] F. Derrien, J. F. Heninot, M. Warenghem, and G. Abbate, *J. Opt. A* **2**, 332 (2000).
- [25] M. Warenghem, J. F. Blach, and J. F. Heninot, *J. Opt. Soc. Am. B* **25**, 1882 (2008).
- [26] R. Dabrowski, J. Dziaduszek, and T. Szczucinski, *Mol. Cryst. Liq. Cryst.* **124**, 241 (1985).
- [27] J. Li, S. Gauza, and S. T. Wu, *J. Appl. Phys.* **96**, 20 (2004).
- [28] S. Jungling and J. C. Chen, *IEEE J. Quantum Electron.* **30**, 2098 (1994).
- [29] A. A. Hardy and W. Streifer, *IEEE J. Lightwave Technol.* **3**, 1135 (1985).
- [30] R. Gati and M. K. Oberthaler, *J. Phys. B: At. Mol. Opt. Phys.* **40**, R61 (2007).
- [31] Y. Silberberg and G. I. Stegemen, *Appl. Phys. Lett.* **50**, 801 (1987).
- [32] M. Matuszewski, B. A. Malomed, and M. Trippenbach, *Phys. Rev. A* **75**, 063621 (2007).
- [33] I. Kaminer *et al.*, *Opt. Lett.* **32**, 3209 (2007).